Internal Bremsstrahlung Spectrum Accompanying 1S Electron Capture in Decay of Fe^{55}, Cs^{131}, and Tl^{204}†

M. H. Biavati, S. J. Nassiff,* and C. S. Wu
Columbia University, New York, New York

(Received October 2, 1961)

The internal bremsstrahlung spectra in coincidence with the K x rays resulting from $1S$ electron capture in Fe^{55} and Cs^{131} have been measured. The results are in good agreement with Martin and Glauber's revised calculations including relativistic and screening effects. The shape of the coincidence spectra exhibits a maximum at the predicted energy and then drops off in intensity toward the low-energy region. This is markedly different from that of the total bremsstrahlung spectrum, which rises continuously toward the low-energy region. In the case of Cs^{131}, the shape of the bremsstrahlung spectrum pertaining to the radiative capture of P electrons as obtained by subtracting from the total spectrum the spectrum due to S-electron capture is also in good accord with that predicted. An estimate of the total probability for bremsstrahlung production during $1S$ electron capture as obtained by comparing the corresponding bremsstrahlung spectrum with the x-ray intensity gives $(1.5\pm0.8)\times10^{-5}$ for Fe^{55} and $(1.4\pm1)\times10^{-5}$ for Cs^{131}, which is in fair agreement with the theoretical prediction including relativistic corrections. The end point of the $1S$ electron capture bremsstrahlung spectrum of Tl^{204} was also measured and found to be 310 ± 10 kev.

I. INTRODUCTION

THE total internal bremsstrahlung spectra accompanying the electron capture decay of many nuclei have been investigated. In every case the intensity distribution exhibits a steep rise as the characteristic x-ray energy is approached. This is in disagreement with early theoretical calculations[1] which predict a decrease in intensity in this low-energy region. Recent considerations,[2] however, show that the observed intensity increase in the low-energy region of the total bremsstrahlung spectrum is due to capture of P-state electrons. In the early calculations the angular momentum of the electron in its initial state was neglected and free-particle wave functions were used for the electron in its intermediate state.

This research was undertaken to provide experimental confirmation of the recent calculation relating the relativistic theory to the bremsstrahlung from $1S$ and $2P$ capture independently, as presented by Glauber and Martin.[3] Experimental confirmation of the shape of the total bremsstrahlung spectrum with relativistic and screening corrections applied has been obtained for several nuclei, namely Ar^{37},[4] V^{49},[5] and[6] Sb^{119} as shown in reference 3. Agreement with the theoretical predictions is excellent down to energies approaching that of the characteristic x ray. Qualitative agreement with the early nonrelativistic theoretical predictions[2] concerning the shape of the spectrum accompanying $1S$ electron capture alone has been obtained for Cs^{131} down to 50 kev by Michalowicz.[7] The shape of the partial spectrum (that due to $1S$ electron capture alone) is, however, not very sensitive to the relativistic corrections. No estimate of the ratio of radiative to nonradiative $1S$ electron capture is given there, and this is very sensitive to the relativistic corrections.

The technique used is to measure only that bremsstrahlung which is in coincidence with the characteristic K x rays emitted as a result of capture of a $1S$-state electron. This affords a means of separation of the bremsstrahlung accompanying S-electron capture from that accompanying capture from states of higher angular momentum. If the Glauber and Martin theory is correct, the steep rise in intensity at low energies should be absent from this coincidence spectrum. The shapes of the spectra thus obtained are compared with the theoretical predictions. An estimation of the probability of bremsstrahlung production during $1S$ electron capture is also given and compared with the relativistic theory. The nuclei which were investigated, Fe^{55} and Cs^{131}, are of particular interest since they have only one decay mode, namely, electron capture. The available energy for the electron capture decay, which is equal to the mass difference between the initial and final nucleus plus the rest mass of the electron minus its binding energy, is less than $2m_0c^2$ and is therefore insufficient to permit positron emission to occur. These two isotopes are also ideally suited to the investigation because of the fact that there are no monoenergetic gamma rays accompanying their decay, as both capture processes go directly to their ground states.

In addition, an investigation of the high-energy region of the internal bremsstrahlung spectrum associated with electron capture in Tl^{204} was made for the purpose of determining the end point and thus the available energy for the decay. The result obtained is compared with those of previous investigators.

II. THEORETICAL BACKGROUND

Radiative electron capture is a second-order process in which an electron in a bound state undergoes a radiative transition to an intermediate state from which

† This work was partially supported by the U. S. Atomic Energy Commission.

* Now at Comision Nacional de Energia Atomica, Buenos Aires, Argentina.

[1] P. Morrison and L. I. Schiff, Phys. Rev. **58**, 24 (1940).
[2] R. J. Glauber and P. C. Martin, Phys. Rev. **95**, 572 (1954).
[3] P. C. Martin and R. J. Glauber, Phys. Rev. **109**, 1307 (1958).
[4] T. Lindqvist and C. S. Wu, Phys. Rev. **101**, 905 (1956).
[5] R. W. Hayward and D. D. Hoppes, Phys. Rev. **104**, 183 (1956).
[6] J. L. Olsen, L. G. Mann, and M. Lindner, Phys. Rev. **106**, 985 (1957).
[7] A. Michalowicz, Compt. rend. **242**, 108 (1956).

it is then captured by the nucleus. The probability per unit time for the process is given by the expression:

$$\omega_k dk = \frac{2\pi}{\hbar}\rho_\nu(W-k)\rho_\gamma(k)dk \times\left|\sum_i \frac{(f|H|i)(i|\gamma_\mu A_\mu|0)}{E_0-E_i}\right|^2. \quad (1)$$

This corresponds to the emission of a gamma quantum with an energy between k and $k+dk$, where ρ_ν and ρ_γ are the density of the final neutrino and γ-ray states per unit energy, respectively. W is the available energy for the interaction and H is the Hamiltonian for the capture of the electron by the nucleus. γ_μ refers to a component of the Dirac anticommuting matrices and A_μ is the radiation field operator corresponding to photon creation. i refers to the intermediate states and 0 to the original states. The summation extends over all intermediate states, bound and continuous.

Early attempts[1] to calculate the intensity and shape of the gamma spectrum accompanying electron capture led to a distribution of the form $x(1-x)^2$, where x is the ratio of the gamma-ray energy to the available energy for the reaction. The result was obtained by using free-particle wave functions for the intermediate S states and by neglecting the angular momentum of the electron in its initial state. Experimental results[8–10] show deviations from the above distribution particularly in the low energy region where the intensity increases with decreasing photon energy in obvious disagreement with the above prediction. The inadequacy of the theoretical calculation is due to the lack of consideration of the fact that the actual process takes place in a region

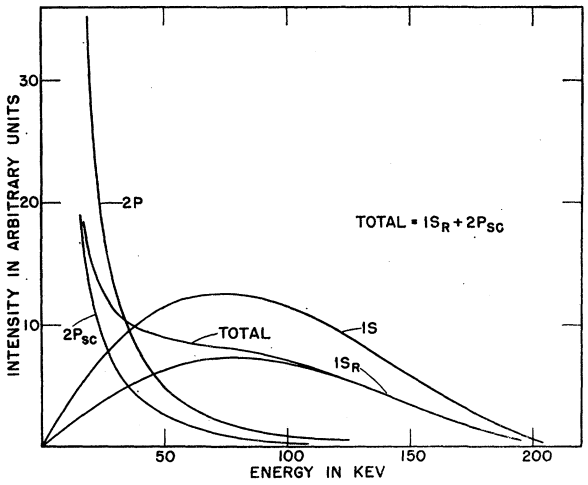

FIG. 1. Fe^{55} theoretical results calculated from Martin and Glauber (reference 3), with relativistic Eqs. (4.3), (4.4) and screening corrections. The curves $1S$ and $2P$ are the uncorrected spectra.

[8] L. Madansky and F. Rasetti, Phys. Rev. **94**, 407 (1954).
[9] W. S. Emmerich, S. E. Singer and J. D. Kurbatov, Phys. Rev. **94**, 113 (1953).
[10] B. Saraf, Phys. Rev. **94**, 642 (1954).

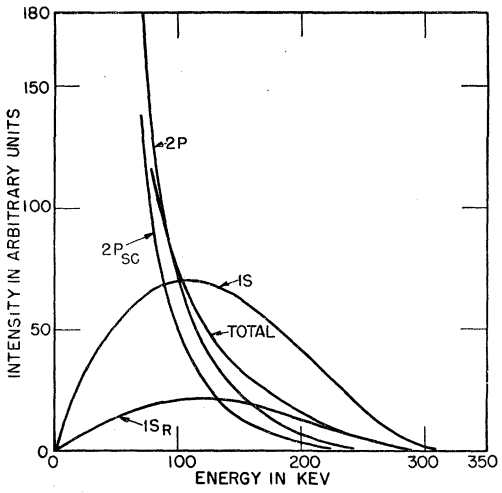

FIG. 2. Cs^{131} theoretical results calculated in the same manner as for Fe^{55}.

where the Coulomb field is very intense, and thus it cannot be ignored, except for very high energy gamma rays and for nuclei of low Z.

A more general treatment of the problem is given by Glauber and Martin.[11] They employ bound-state wave functions for the initial states of the electron. The summation over the intermediate states of the electron is done in the presence of the Coulomb field of the nucleus. The summation is shown to be implicitly contained in the Green's function satisfying an inhomogeneous form of the Schrödinger equation.

The result obtained for the transition rate for radiative capture from an S shell predicts the same spectrum shape as that obtained by Morrison and Schiff; namely, it has the form $k(k_{\max}-k)^2$. It thus exhibits the steady decrease in intensity as the characteristic x-ray energy is approached. The major contribution to the low-energy part of the spectrum is due to capture of P-state electrons. In this case the Green's function which embodies the summation over the intermediate states has a pole at the characteristic x-ray energy. This accounts for the sharp increase in intensity in the low-energy region. It is also to be noted that the ratio of radiative P capture to nonradiative capture is proportional to Z^2 and therefore for a given $k_{\max}$ the P-state spectra intensity increases as Z^2 relative to the S-state spectra. The theoretical results for $1S$ and $2P$ electron capture for Fe^{55} and Cs^{131} are given in Figs. 1 and 2, curves $1S$ and $2P$.

A complete relativistic treatment of the problem is given in reference 3. Relativistic electron wave functions for the Dirac equation are employed throughout. The summation over intermediate states is represented by a Green's function for the Dirac equation in a Coulomb field. The relativistic corrections are applied directly to the innermost S-state electron bremsstrahlung spectrum. They are negligible for the P-state electrons

[11] R. J. Glauber and P. C. Martin, Phys. Rev. **104**, 158 (1956).

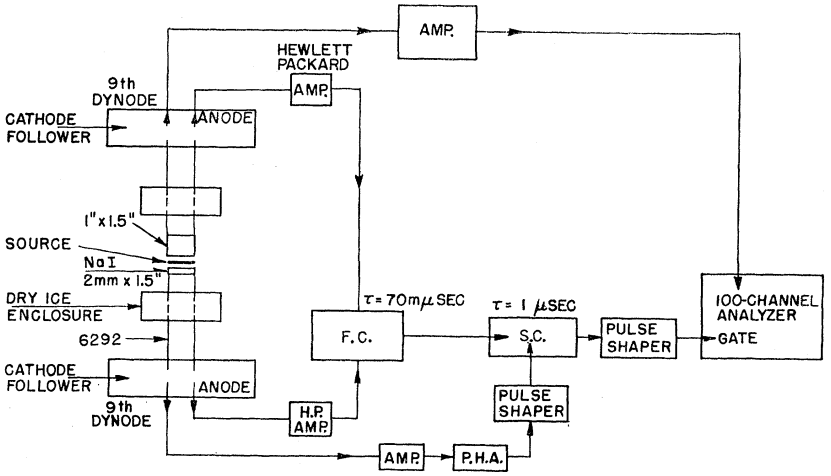

FIG. 3. Schematic diagram of apparatus.

because the Coulomb field has a smaller effect. Most of the bremsstrahlung from P-electron capture is low in energy, and as a result, relativistic corrections are not as important as are screening corrections.

The probability for bremsstrahlung production as a result of capture of a $1S$ electron, compared with the probability for nonradiative K capture, is given by the expression,

$$\frac{W_{1S}}{W_c}=\frac{\alpha}{\pi m^2}\int_0^{(k_{\max})_{1S}} k\left(1-\frac{k}{(k_{\max})_{1S}}\right)^2 R_{1S}(k)dk, \quad (2)$$

where α is the fine structure constant. This is identical to the Morrison and Schiff results except for the relativistic factor $R_{1S}(k)$ which reduces the over-all intensity of the spectrum but does not appreciably affect the shape. The fully corrected spectra including relativistic and screening effects for Fe^{55} and Cs^{131} are given in Figs. 1 and 2, curves $1S_R$ and $2P_{sc}$. The relativistic correction was obtained from Eq. (4.3 a, b) of reference 3 with the aid of the IBM–650 computer. The screening correction which was applied to the $2P$ state spectra is given in reference 3 also. The most important effect of screening is to reduce the $2P$ spectrum relative to the $1S$ spectrum. This effect is larger when Z is small.

III. EXPERIMENTAL APPARATUS

A schematic of the apparatus used throughout the experiment is given in Fig. 3. Two scintillation counters are used to detect the x rays and bremsstrahlung. The pulses from the anode of each photomultiplier tube are amplified by two Hewlett-Packard wide-band amplifiers and then fed to a fast coincidence unit of variable resolving time. The signal from the ninth dynode of the photomultiplier used to detect the bremsstrahlung photons is fed to a nonblocking linear amplifier (Hamner model No. 301) of high gain and its output then connected to a 100-channel pulse-height analyzer. The ninth dynode output of the photomultiplier tube used to detect the x rays is amplified with a similar amplifier and then analyzed on a pulse-height selector which is adjusted to pass only those pulses corresponding to the characteristic K x-ray energy. This K x-ray output is then properly shaped and fed to a slow-coincidence unit along with the output of the fast-coincidence circuit. The output of the slow coincidence is eventually applied to gate the 100-channel analyzer on which the coincidence bremsstrahlung spectrum is displayed. For the detection of the K x rays (5.9 kev) resulting from $1S$ electron capture in Fe^{55}, a sodium iodide crystal (80 mils thick, 1.5 in. in diameter) sealed in a container with a thin window of 5-mil beryllium and a 100-μg/cm^2 aluminum reflector was used. A resolution of 50% (defined as the full width of the intensity distribution at half maximum) was obtained for the 5.9-kev manganese x ray. The x ray resulting from $2P$ electron capture is less than 1 kev and does not appreciably penetrate the beryllium window. The absorption of the soft 5.9-kev x rays in the beryllium window is less than 5%. Background was reduced by surrounding both detectors on all sides with $1\frac{1}{2}$-in. lead lined with 0.25 in. copper to absorb lead x rays and 0.25 in. aluminum to absorb copper x rays. The lead was placed so as not to be closer than 6 in. from the crystals at any point.

The bremsstrahlung was detected with a 1-in. thick, 1.5-in. diameter sodium iodide crystal with a 0.5-mil aluminum window. A resolution of 30% was obtained for the 29-kev iodine x rays. Sources of Cs^{137} (31-kev x ray), Bi^{207} (77 kev), and Se^{75} (138 and 269 kev) were used for calibration. The relation between the energy and pulse height was linear in the energy region investigated which, in the case of Fe^{55}, was from the maximum of 220 kev down to 20 kev. Because of the necessity to make measurements of such low-energy pulses, it was necessary to use dry ice to cool down the photomultiplier tubes in order to decrease the noise background. However, it was observed that cooling of the crystals (by conduction) caused a loss in pulse height around 40%, so a 1-in. long and 1.5-in. diameter Lucite light guide was placed between the photomulti-

plier and the crystal. The loss in pulse height is probably due to the indirect consequence of an increase in the decay time of the crystal with decrease in temperature,[12] and results from clipping the pulses at the anode of the photomultiplier to reduce pulse pileup. The over-all loss in pulse height due to cooling and Lucite light guide together was only 20% as compared to 40% without the light guide.

The fast coincidence resolving time T was 70 mμsec for Fe^{55} (T being defined as the half-width at half maximum of the time resolution curve). This gave a coincidence efficiency of almost 100% (Fig. 4) as is evident from the flatness of the time resolution curve. The true-to-accidental ratio obtained was 4:1. The delay which was inserted in order to measure the accidentals was placed between the anode of the bremsstrahlung detector and the wide band (Hewlett-Packard in Fig. 3) amplifier. It represented a time delay of 150 mμsec.

It is of great importance for this experiment to ascertain that the efficiency of the electronics not be a function of the pulse height, in particular with regard to the bremsstrahlung pulses. In relation to this, the time resolution curve was measured as a function of pulse height in order to detect any possible shift. This was accomplished by measuring the curve as a function of the discriminator level setting for the bremsstrahlung pulses at the input of the fast coincidence unit. Two such curves are presented in Fig. 4. One corresponds to the minimum level setting used throughout the experiment and the other to a setting corresponding to half the maximum limiting pulse height. The shift is seen to be negligible.

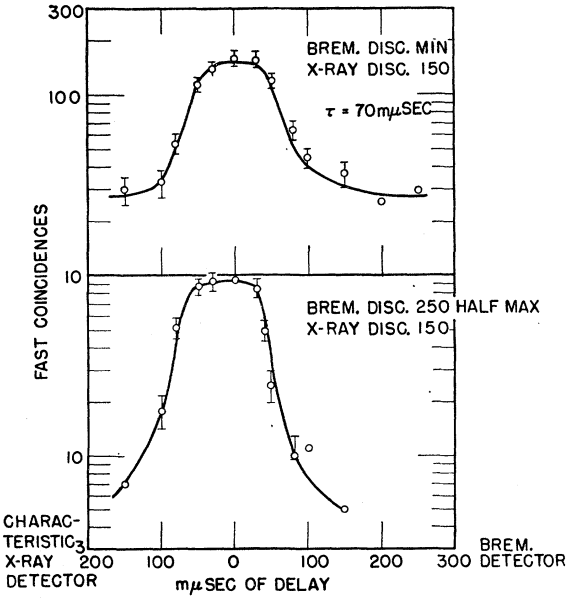

FIG. 4. Fast coincidence time resolution curve as a function of pulse height for Fe^{55}.

[12] J. Bonanomi and J. Rossel, Helv. Phys. Acta **25**, 725 (1952).

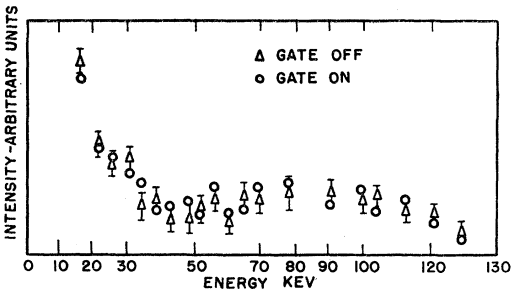

FIG. 5. Gated and ungated total spectra for checking efficiency of electronics as a function of energy.

Another experimental check to test the uniformity of the efficiency of the apparatus is related to a possible effect caused by setting the discriminator for the bremsstrahlung pulses at the input of the fast coincidence unit too high. It is desirable to set this level as high as possible to discriminate against the noise. However, if it is set too high it will also discriminate against the lower energy bremsstrahlung pulses, giving rise to a fictitious decrease in intensity. It is just such a decrease in intensity which the experiment seeks to confirm (note theoretical bremsstrahlung spectrum for 1S electron capture). The procedure used to determine the proper discriminator setting is the following. The output pulses from the Hewlett-Packard wide band amplifier in the bremsstrahlung branch was connected simultaneously to both inputs of the fast coincidence circuit. A fast coincidence pulse is then obtained for all pulses above the discriminator level setting. This output is then used to gate the multichannel analyzer. The gated total bremsstrahlung spectrum thus obtained is then compared with the ungated total spectrum. Both curves are given in Fig. 5. They are in agreement within the statistical error down to 17 kev. In order to measure accidental coincidences a cable of 150-mμsec delay for Fe^{55} was placed between the output of the bremsstrahlung cathode follower and the wide-band amplifier. The gain of the amplifier was raised in order to account for the attenuation of the cable. These checks served to prove that the coincidence efficiency of the electronics was independent of pulse height down to 17 kev at least.

IV. Fe^{55}

The bremsstrahlung spectrum corresponding to capture of a 1S electron was measured. Fe^{55} decays by pure electron capture with a half-life of 2.6 years to the ground state of Mn^{55}. About 70% of the atomic excitation after electron capture gives rise to Auger electron emission and the remainder to x-ray emission. The L_1/K capture ratio is given as 0.09.[13] The decay is characterized by a logft value of 6.1 and is allowed but unfavored since $\Delta L=2$. The source was obtained from Oak Ridge

[13] H. Brysk and M. E. Rose, Oak Ridge National Laboratory Report ORNL-1830, 1955 (unpublished).

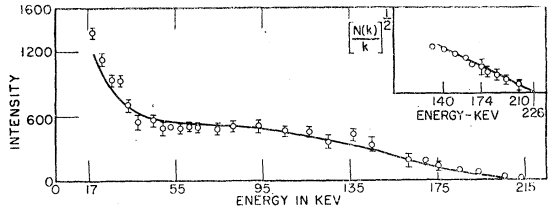

FIG. 6. Fe^{55} total bremsstrahlung spectrum. Solid curve gives predicted spectrum from Glauber and Martin. Insert shows analogous Kurie plot of end point.

and was made by neutron irradiation of an enriched sample of Fe^{54}.

Impurities of manganese and cobalt were separated out chemically by using repeated processes of paper chromatography.[14] The absence of the characteristic gamma rays accompanying the decay of these nuclei was evidence that the purification was better than one part in 10^6. The chemistry was performed about five years after the irradiation to assure the complete decay of Fe^{59} which has a half-life of 45 days. The absence of the 1.098- and 1.289-Mev gamma rays which accompany the decay of Fe^{59} indicated its complete decay. The intensity of the source used was $\sim 1.0\times 10^5$ disintegrations/sec.

The experimental points for the total bremsstrahlung spectrum are given in Fig. 6. The points have been corrected for background and crystal efficiency, including the solid-angle factor. An analogous Kurie plot of the upper energy portion of the spectrum gives an end point of 220 ± 10 kev which is in agreement with previous results.[15] The Kurie plot is obtained by plotting $[N(k)/k]^{\frac{1}{2}}$ against k (photon energy). The total spectrum shows the steep rise in intensity at low photon energies and is in good agreement with the total spectrum predicted from Glauber and Martin theory (solid curve in Fig. 6). The spectrum in coincidence with the 5.9-kev manganese x rays is given in Fig. 7. The

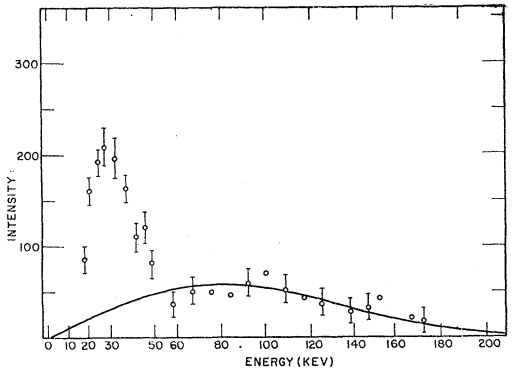

FIG. 7. Fe^{55} coincidence spectrum. Solid curves give predicted spectrum from Glauber and Martin.

solid curve represents the theoretical prediction of Glauber and Martin. A definite peak at ~ 29 kev is seen to be present. The decrease in intensity below this energy is not a result of energy dependence of the coincidence efficiency of the electronics, as was previously discussed. The coincidence data have been corrected for accidentals and true background coincidences. The shape of the accidental spectrum was the same as that of the total bremsstrahlung spectrum, as expected. The ratio of source true coincidences to background true coincidences was 6:1. The coincidence spectrum has also been corrected for escape of iodine x rays from the bremsstrahlung crystal[16] and for solid angle and crystal efficiency. Correction for absorption of bremsstrahlung in the 0.5-mil aluminum window is negligible and was not applied. The transmission in the 0.5-mil Al window is greater than 98% for 20-kev photons.

Considering the geometry used in the experiment, the origin of the peak at ~ 29 kev might be due to the iodine escape x rays (29 kev) resulting from photoelectric absorption of bremsstrahlung in the 80-mil x-ray crystal. The probability for escape of an iodine x ray from a sodium iodide crystal as a function of photon energy k is given by Novey.[16] For low-energy photons (greater than 34 kev which is the K edge of iodine) the interaction in the sodium iodide crystal is mostly due to the photoelectric effect and occurs mainly near the crystal surface. The escape probability of an iodine x ray from an 80-mil sodium iodide crystal for low-energy photons is very considerable. The escaped x rays which reach the bremsstrahlung-detecting crystal will register as a coincidence count with the photoelectron pulses left behind in the x-ray crystal. The escaping iodine x-ray intensity which was detected in the bremsstrahlung detector seemed to be disproportionately large compared to the observed coincident bremsstrahlung. This was due to the fact that 70% of the atomic de-excitation following electron capture in Fe^{55} proceeds by way of Auger electron emission and only the remaining 30% by characteristic K x-ray emission. This reduces the true coincidences between the bremsstrahlung and the K x ray accordingly. Absorption of the 5.9-kev x rays in the source material itself will also add to this distorted effect.

The order of magnitude of this iodine x-ray escape effect can be estimated. The window of the pulse-height analyzer in the x-ray branch is opened to accept pulses of 5.9 kev in energy, but due to the poor resolution in the low-energy region, photons of 4 to 12 kev will also be passed. Since the iodine x-ray energy is 29 kev, bremsstrahlung in the energy range 33–41 kev will be responsible for the coincidences contributing to the peak. To estimate the order of magnitude of this effect the intensity of the total bremsstrahlung spectrum in the above energy region is obtained. This is then multiplied by the probability for escape and the solid angle

[14] E. and M. Lederer, *Chromatography* (Elsevier Publishing Company, Inc., Amsterdam, 1953), 1st ed.

[15] D. Strominger, J. M. Hollander, and G. T. Seaborg, Revs. Modern Phys. **30**, 713 (1958).

[16] T. B. Novey, Phys. Rev. **89**, 672 (1953).

for detection of the iodine x ray by the bremsstrahlung crystal. The result was in good agreement with the area under the peak observed in the coincidence spectrum, assuming 100% coincidence efficiency.

To check further whether the above is the correct interpretation for the observed coincidence peak, a graded x-ray shield consisting of indium foil (5 mils) which has a high mass absorption coefficient for 29-kev x rays, sandwiched between brass foil (5 mils) and aluminum foil (8 mils) was prepared. A hole $\frac{5}{16}$ inch in diameter was cut in the center for the Fe^{55} source. This arrangement should have no effect on the total spectrum. The measured total spectra with and without the shield are given in Fig. 8 and are in agreement within the statistical fluctuation. The coincidence spectrum with the shield is given in Fig. 9. The coincidence peak around 29 kev was greatly reduced with the shield (a factor of 6). This supports the correctness of the interpretation of the observed peak.

Further confirmation was obtained by an independent and supplementary measurement in which a Cs^{137} source uniformly spread over an extended area of the size of the x-ray crystal was placed at the position of the

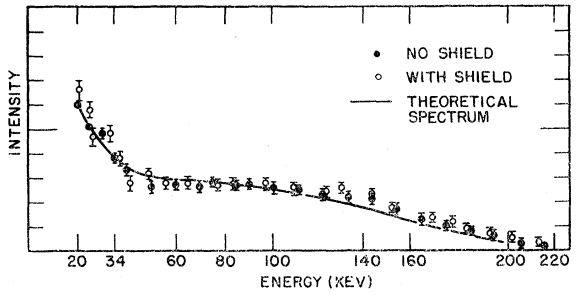

FIG. 8. Fe^{55} total spectrum with and without shield for stopping iodine x ray. Solid curve gives theoretical prediction of Glauber and Martin.

crystal. The barium x ray from Cs^{137} was then measured in the bremsstrahlung crystal with and without the graded shield. A reduction in intensity of a factor of 6 was again found in this case and thus gives strong support to the interpretation. The observed shape of the barium x-ray peak with the graded shield in position was then used to correct for the iodine escape x ray passing through the hole of the shield.

After applying this correction, the coincidence bremsstrahlung spectrum is in excellent agreement with that predicted theoretically by Glauber and Martin from 20 kev to the upper energy limit (Fig. 10).

A calculation of the probability of radiative $1S$ electron capture was made by comparing the bremsstrahlung intensity with the x-ray intensity (corrected for Auger electron emission). The bremsstrahlung intensity was calculated by obtaining the area under the coincidence spectrum corrected for crystal efficiency, solid angle, and iodine x-ray intensity and extrapolating the curve to the low-energy region below 20 kev on the

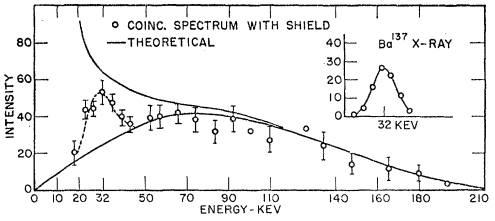

FIG. 9. Fe^{55} coincidence spectrum with shield. Solid curves give the theoretical prediction of Glauber and Martin for the total and $1S$ capture spectra.

basis of the theoretical predictions. This yields a value of $(1.5\pm0.8)\times10^{-5}$ as compared to the theoretical prediction of 2.0×10^{-5} (considering the relativistic correction). The agreement is fair.

The theoretical calculations were made using the result given for W_{1S}/W_C in Eq. (2). The distribution $k(1-k/k_{\max})^2R_{1S}(k)$ was plotted versus k using the numerical values for $R_{1S}(k)$ obtained from Eq. (4.3 a,b) of reference 3. The integration was done by taking the area under the curve. The actual ratio W_{1S}/W_C of radiative to nonradiative capture of $1S$ electrons was obtained by multiplying the area by $\alpha/\pi m^2$ as required in Eq. (2). Screening of $1S$ electrons was taken into consideration, but is, however, small. For the case of Fe^{55} an end-point $k_{\max}$ of 220 kev was used.

V. Cs^{131}

For the investigation of the internal bremsstrahlung spectrum in coincidence with the x rays resulting from $1S$ electron capture in Cs^{131}, some changes in the experimental arrangement were made. It was not necessary to cool the photomultiplier tubes since the xenon K x-ray energy is 29.8 kev. As a result of not having to cool the tubes to dry ice temperature, there was no necessity for using the 1-in. Lucite light pipes. The resolving time of the fast coincidence circuit was improved from 70 to 20 mμsec (Fig. 11) and a true-to-accidental ratio of 20:1 was obtained. The curve for the fast resolving time is presented for two values of the discriminator level setting. These is no significant shift as a function of discriminator level and thus the curves are independent of photon energy. With the resolving

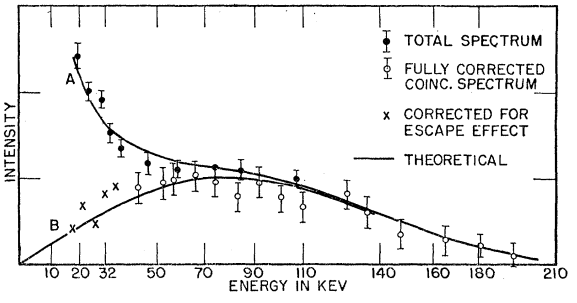

FIG. 10. Fe^{55} fully corrected total and coincidence spectra and comparison with theoretical results. Crosses represent experimental data corrected for iodine x ray.

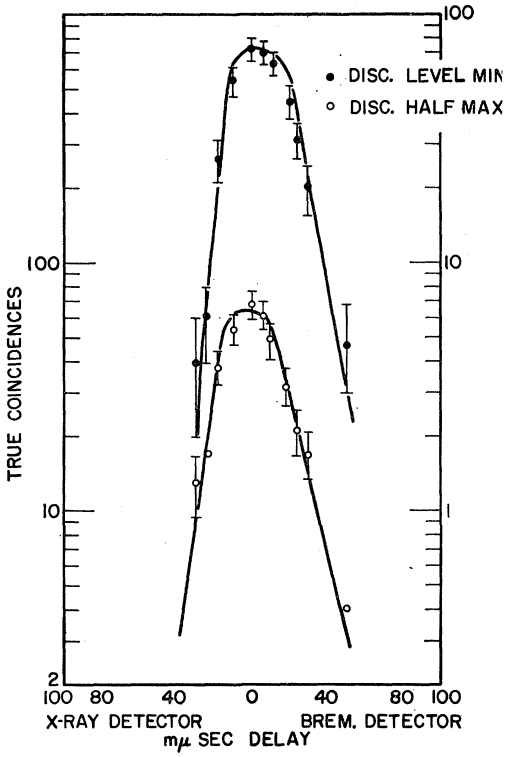

FIG. 11. Cs^{131} fast coincidence time resolution curve as a function of pulse height.

time used, the coincidence efficiency is close to 100%. This is estimated by measuring the fall of the fast coincidence rate with time delay (Fig. 11) or in other words, by measuring the slope of the true coincidence time delay curve. A copper absorber 50 mils thick was placed between the source and bremsstrahlung crystal so that x-ray pileup in the crystal would be greatly reduced. All the data have been corrected for this absorption. For the detection of the bremsstahlung a sodium iodide crystal 1-in. diameter by 1 in. thick with a 0.5-mil aluminum window was used. For the x-ray detector a 1.5-in. diameter, 80-mil thick sodium iodide crystal with 0.5-mil aluminum window was used. Absorption of the x ray and lower energy bremsstrahlung in the 0.5-mil aluminum window is negligible. The source to crystal distance was 0.106 in. A resolution of 30% for the 138-kev gamma ray of Se^{75} for the bremsstrahlung crystal was obtained. For calibration purposes the 31-kev x ray of Ba^{137} and the gamma rays of RaD (47 kev), Bi^{207} (74.8 kev), and Se^{75} (138 kev and 269 kev) were used.

To check the relative coincidence efficiency versus energy a Ba^{131} source was used. This source is particularly useful because it decays by pure electron capture to an excited state of Cs^{131} which decays to the ground state with the emission of gamma rays of energy 42, 82, 122, 214 kev. Therefore, the total ungated spectrum can be measured and compared with the spectrum in coincidence with the 31-kev x ray to determine whether there is any change in coincidence efficiency with energy. This arrangement approximates the actual experimental situation with the Cs^{131} very closely. The ungated and gated spectra are given in Fig. 12. The ratio of the areas of corresponding gamma rays is constant as a function of energy down to 42 kev. This shows that the over-all coincidence efficiency is independent of energy.

Cs^{131} has a half-life of 9.6 days.[15] It decays by pure electron capture to the ground state of Xe^{131} with the emission of the characteristic Xe x rays. The probability for Auger electron emission is small. (K fluorescence yield is 0.87.)[17] The internal bremsstrahlung spectrum has an end point at 320±10 kev.[18] Previous measurements of the total spectrum show the usual rise as the energy decreases, in direct contradiction to the Morrison and Schiff results.[19,20] This effect is particularly noticeable for Cs^{131} since it has a high Z. The probability of bremsstrahlung emission during $2P$ electron capture as compared to that accompanying $1S$ electron capture is proportional to Z^2.

The source was grown out of the electron capture decay of Ba^{131}. The Ba^{131} was obtained from Oak Ridge

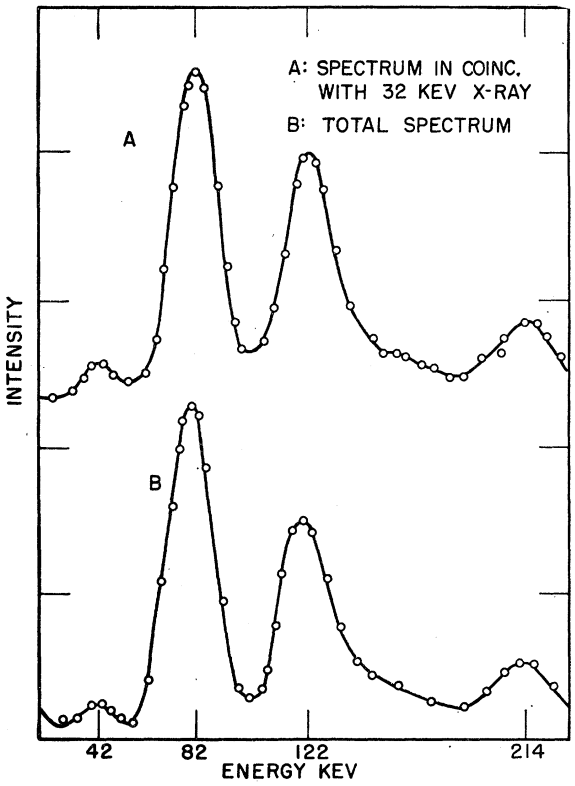

FIG. 12. Ba^{131} total and coincidence spectrum for determining efficiency of electronics as a function of energy.

[17] K. Siegbahn, *Beta- and Gamma-ray Spectroscopy* (North Holland Publishing Company, Amsterdam, 1955), p. 630.
[18] B. Saraf, Phys. Rev. **94**, 642 (1954).
[19] D. D. Hoppes and R. W. Hayward, Phys. Rev. **104**, 368 (1956).
[20] L. Lidofsky, P. Macklin, and C. S. Wu, Phys. Rev. **87**, 391 (1952).

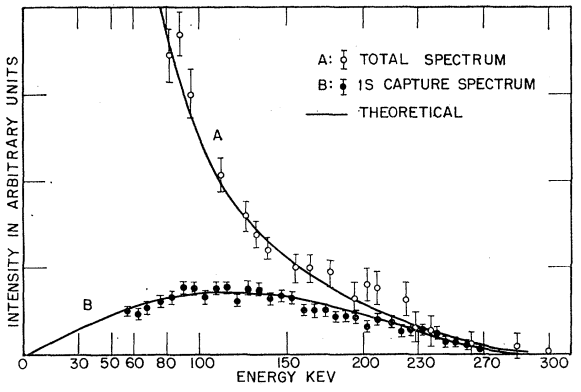

FIG. 13. Cs^{131} fully corrected total and coincidence spectra and comparison with theoretical predictions.

National Laboratory, where it was made by irradiating Ba^{130} with neutrons from a pile.

$$Ba^{130}(n,\gamma) \rightarrow {}_{56}Ba^{131} \xrightarrow[12\text{ days}]{K\text{ capture}} {}_{55}Cs^{131} \xrightarrow[9.6\text{ days}]{K\text{ capture}} {}_{54}Xe^{131},$$

which is stable. Cs^{132} was also present in the source as an impurity [from $Ba^{132}(n,p)$] and was separated out by the paper chromatography method (Lederer).[14] The Ba^{131} decays to Cs^{131} by electron capture with a half-life of 12 days. Ten days after the Cs^{132} was separated from the barium, another separation was made to obtain the pure Cs^{131}. The procedure was followed by precipitation in order to complete the separation of Ba^{131}.[19] The separation of Ba^{131} was better than 1 part in 10^6. None of the characteristic gamma rays of Ba^{131} was observed. The only observable impurity was a radioactive substance of long half-life (no decrease in activity observed for one month) with a gamma ray of $\sim$500 kev which was found not to be in coincidence with the Ba x-ray. The contribution of the impurity to the total bremsstrahlung spectrum was obtained by measuring the total spectrum of the source one month after the total and gated spectra of the Cs^{131} were first obtained. The Cs^{131} has thus decayed to one-tenth of its original intensity. The total bremsstrahlung spectrum is given in Fig. 13 by the open circles. It has been corrected for the impurity, for background, for absorption in the copper, and for crystal efficiency. The spectrum in coincidence with the 29.9-kev x ray is given in Fig. 13 by the solid dots. The solid curve gives the result of the fully corrected (relativistic and screening) Glauber and Martin theory. The difference between the total spectrum and $1S$ capture spectrum has been plotted (normalizing at high energy where contribution from $2P$ capture is small) in Fig. 14. This represents the spectrum from $2P$ electron capture only. The contribution from nS ($n>1$) and nP ($n>2$) capture is negligible. The agreement with theory is very good. The probability for bremsstrahlung emission from $1S$ electron capture can be calculated by comparing the total $1S$ bremsstrahlung intensity with the x-ray intensity in the same manner as for Fe^{55}. This gives a value of $(1.4\pm1)\times10^{-5}$, which is in agreement with the Martin and Glauber prediction of 2.2×10^{-5}, taking into consideration rigorous relativistic effects.

As was previously discussed, qualitative agreement with the nonrelativistic calculations of the theory has already been obtained by Michalowicz,[7] who measured coincidences between the x ray resulting from 1 S electron capture and the bremsstrahlung. No quantitative estimate of the bremsstrahlung emission per electron capture decay was made there.

VI. Tl^{204}

An investigation of the end point of the internal bremsstrahlung spectrum associated with $1S$ electron capture in Tl^{204} was made by using the coincidence technique previously discussed. Tl^{204} decays in two modes with a half-life of about 4 years. 98% of the decay proceeds by electron emission to the ground state of Pb^{204} with an end point of 760 kev.[21] The remainder of the decay proceeds by electron capture to stable Hg^{204}. Previously reported end points for the internal bremsstrahlung associated with the capture are 250 kev[21] and 290 ± 20 kev.[22] Tl^{204} was obtained from Oak Ridge National Laboratory. The absence of any monochromatic gamma-rays indicated that there was no need for chemical purification. The end point of the internal bremsstrahlung spectrum was determined by measuring coincidences between the 70.8-kev Hg^{204} x rays resulting from $1S$ electron capture and the in-

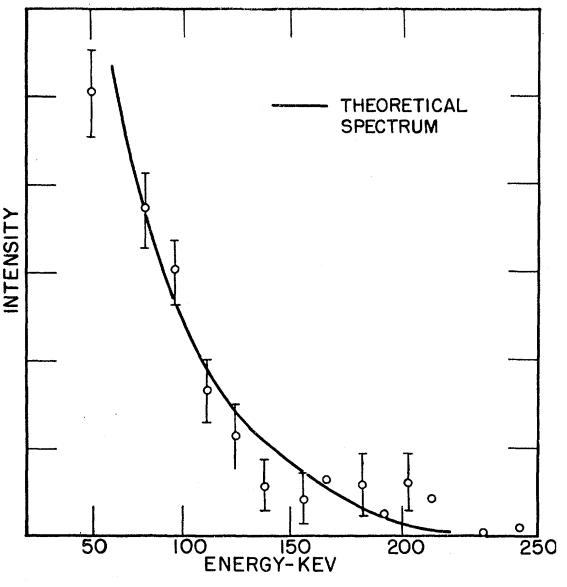

FIG. 14. Cs^{131} total minus $1S$ coincidence spectrum. Solid curve represents the Glauber and Martin predicted spectrum for $2P$ electron capture.

[21] E. der Mateosian and A. Smith, Phys. Rev. 88, 1186 (1952).
[22] R. Jung and M. L. Pool, Bull. Am. Phys. Soc. 1, 1172 (1956).

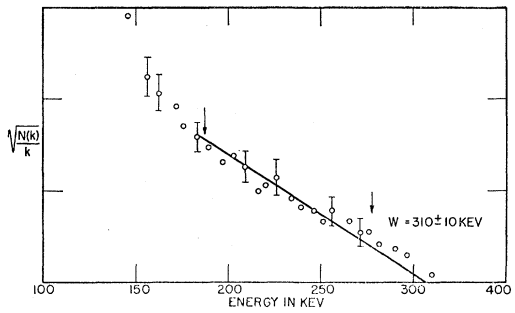

FIG. 15. Tl^{204} Kurie plot of high-energy and of coincidence spectrum.

ternal bremsstrahlung. Because of the high branching ratio for beta decay compared to capture and also to reduce pile-up of the x ray, it was necessary to place a 0.1-in. copper disk between the source and bremsstrahlung-detecting crystal and a 0.13 in. thick Lucite disk between the source and x-ray crystal. (The latter is to absorb preferentially beta rays and not x rays.) The effect of the Lucite disk on the x-ray spectrum is negligible. The resolving time used was 20 mμsec with a true to accidental ratio of 5:1. A 10% resolution for the 660-kev gamma ray of Cs^{137} was obtained with the 1-in.×1-in. sodium iodide bremsstrahlung-detecting crystal. The two crystals were set 2.4 in. apart with the source half-way in between. The absorbers were placed in contact with the crystals. This arrangement was chosen in order to make the probability for the occurrence of true coincidences arising from scattering of the bremsstrahlung accompanying the electron decay in the copper and crystals as small as possible. Compton scattering of the internal bremsstrahlung accompanying electron capture, near the high-energy end of the spectrum is small, ~15%. A Kurie plot of the coincidence data is given in Fig. 15. The data have been corrected for crystal efficiency and solid angle[23] and absorption. The end point was determined by fitting the data to a straight line by the method of least squares. The end point is 310±10 kev. Using this value, the resolution correction was applied to the data near the end point using the method of Palmer and Laslett.[24] The corrected data are given in Fig. 15 (points above 280 kev).

VII. CONCLUSION

The results which were obtained for Fe^{55} and Cs^{131} show both qualitative and quantitative agreement with the Martin and Glauber predictions. The shape of the bremsstrahlung spectrum which accompanies the capture of 1*S*-state electrons shows the expected drop in intensity at low energies which had already been predicted by Morrison and Schiff in 1940.[1] The spectrum accompanying 2*P* electron capture, on the other hand, accounts for the steep rise in intensity which appears as the characteristic x-ray line is approached (Fig. 14). It is just the presence of this rise in the low-energy portion of the total spectrum which could not be explained on the basis of the early analysis and thus led to the more accurate calculations of Martin and Glauber. The spectra which were obtained in this research for the 1*S*, 2*P* (indirectly), and total bremsstrahlung intensities (Figs. 10, 13, and 14) are in excellent agreement with the theoretical predictions including relativistic and screening factors. The total probability for bremsstrahlung production during 1*S* electron capture as obtained by comparing the corresponding bremsstrahlung spectrum with the x-ray intensity is in fair agreement with the relativistic predictions for both of the isotopes which were investigated.

Isotope	Measured W_{1S}/W_C	Predicted W_{1S}/W_C
Cs^{131}	$(1.4\pm1)\times10^{-5}$	2.2×10^{-5}
Fe^{55}	$(1.5\pm0.8)\times10^{-5}$	2.0×10^{-5}

The limit of accuracy of the measured results is good enough to show agreement with the relativistic predicted values and disagreement with those which are predicted with no consideration of relativistic effects.

The increase in the ratio W_{2P}/W_C with Z^2 is also evident from the data presented in this paper. For Cs^{131} the 2*P* spectrum dominates a large portion of the total intensity, whereas for Fe^{55} it dominates only the very low energy portion.

The result obtained for the end point of the Tl^{204} internal bremsstrahlung spectrum (310±10 kev) is in fair agreement with the value obtained by Jung and Pool[22] of 290±20 kev but is in sharp disagreement with that obtained by der Mateosian and Smith[21] of 250 kev.

ACKNOWLEDGMENTS

The calculations of the theoretical bremsstrahlung spectra were done with the aid of an IBM–650 computer and the authors wish to express their gratitude to the Columbia University Watson Laboratory for the use of the computing facilities.

The authors are particularly indebted to B. J. Biavati for setting up the program for the computer and to M. Glaubman for the design of the coincidence circuitry.

Thanks are due to Mr. W. Herring for his help at the beginning of the experiment.

[23] E. A. Wolicki, R. Jastrow, and F. Brooks, Naval Research Laboratory NRL–4833, 1956 (unpublished).

[24] J. Palmer and L. Laslett, Atomic Energy Commission Report AECU–1220, 1951 (unpublished).